JACS
JOURNAL OF THE AMERICAN CHEMICAL SOCIETY
Article
pubs.acs.org/JACS

6,6-Dicyanopentafulvenes: Electronic Structure and Regioselectivity in [2 + 2] Cycloaddition–Retroelectrocyclization Reactions

Aaron D. Finke,[†] Oliver Dumele,[†] Michal Zalibera,[‡] Daria Confortin,[‡] Pawel Cias,[‡] Govindasamy Jayamurugan,[†] Jean-Paul Gisselbrecht,[§] Corinne Boudon,[§] W. Bernd Schweizer,[†] Georg Gescheidt,[‡] and François Diederich[†,*]

[†]Laboratory of Organic Chemistry, ETH Zurich, Hönggerberg, HCI, CH-8093 Zurich, Switzerland

[‡]Institute of Physical and Theoretical Chemistry, Graz University of Technology, Stremayrgasse 9, A-8010 Graz, Austria

[§]Laboratoire d'Electrochimie et de Chimie Physique du Corps Solide, Institut de Chimie–UMR 7177, C.N.R.S., Université de Strasbourg, 4 rue Blaise Pascal, 67081 Strasbourg Cedex, France

Supporting Information

ABSTRACT: We present an investigation of the electronic properties and reactivity behavior of electron-accepting 6,6-dicyanopentafulvenes (DCFs). The electron paramagnetic resonance (EPR) spectra of the radical anion of a tetrakis-(silylalkynyl) DCF, generated by Na metal reduction, show delocalization of both the charge and unpaired electron to the nitrogens of the cyano moieties and also, notably, to the silicon atoms of the four alkynyl moieties. By contrast, in the radical anion of the previously reported tetraphenyl DCF, coupling to the four phenyl rings is strongly attenuated. The data provide physical evidence for the different conjugation between the DCF core and the substituents in both systems. We also report the preparation of new fulvene-based push–pull chromophores via formal [2 + 2] cycloaddition–retroelectrocyclization reaction of DCFs with electron-rich alkynes. Alkynylated and phenylated DCFs show opposite regioselectivity of the cycloaddition, which can be explained by the differences in electronic communication between substituents and the DCF core as revealed in the EPR spectra of the radical anions.

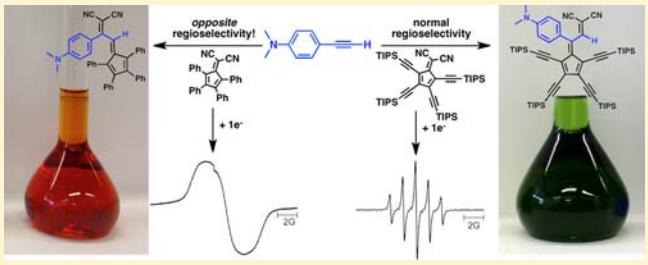

INTRODUCTION

The chemical landscape for organic molecules with desirable properties suitable for application in electronic devices is continuously expanding.[1] While much of the current advancements in organic-based devices use components made of well-established building blocks, breakthroughs in the field of functional organic materials can still result from the discovery of new scaffolds and synthetic methodologies.[2]

To these ends, our research group has developed a new class of nonplanar push–pull chromophores resulting from the formal [2 + 2] cycloaddition–retroelectrocyclization (CA–RE) reaction between electron-rich alkynes and electron-poor olefins.[3] These chromophores have tunable absorption expanding into the near-IR region, display amphoteric redox behavior, and possess reduction potentials which rival those of the linchpin organic acceptors tetracyanoethylene (TCNE) and 7,7,8,8-tetracyano-*p*-quinodimethane (TCNQ).

Much of our work in this area, as well as contributions from other groups,[4,5] has focused on variation of the alkyne donor to modulate the efficiency of donor–acceptor conjugation; the acceptor olefin has been largely limited to TCNE and TCNQ. Only in a few instances have we explored the possibility of tuning the acceptor molecule for this reaction, but these reports have led to some exciting prospects.[6] In particular, the notion arose that *any* sufficiently electron-poor olefin can be potentially reactive in a formal CA–RE reaction with electron-rich alkynes to generate a push–pull system. The next logical step was to identify new acceptors that contain electron-poor olefins and test them for CA–RE reactivity.

Even historically well-studied molecular systems can garner newfound appreciation in novel applications. One such scaffold, pentafulvene, has been investigated for over six decades, and the riches of its chemistry have yet to be exhausted. This isomer of benzene (C_6H_6) has been, and continues to be, a paradigm for the illustration of aromaticity–antiaromaticity to the present day.[7] Although it is a hydrocarbon, pentafulvene has a relatively large dipole moment of 0.44 D[8] owing to its nonbenzenoid connectivity. The positive charge resides on C(6), while the negative charge is delocalized in the five-membered ring. In the highest occupied molecular orbital (HOMO), the electron population resides exclusively in the cyclopentadienyl fragment, while in the lowest unoccupied molecular orbital (LUMO), it can be found at C(6) (Figure 1). Here, we focus our efforts on the underexplored 6,6-dicyanopentafulvenes (DCFs), which have recently found renewed

Received: September 14, 2012
Published: October 8, 2012

 © 2012 American Chemical Society dx.doi.org/10.1021/ja309141r | J. Am. Chem. Soc. 2012, 134, 18139–18146

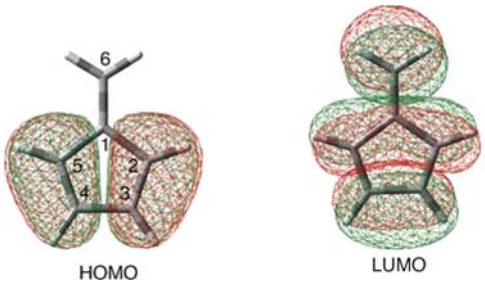

Figure 1. HOMO and LUMO of pentafulvene.

interest as functional materials.[9] Because DCF itself is too reactive to isolate and study, we must rely on stable derivatives.

Andrew et al. have reported the first systematic preparation of stable, phenylated DCFs as n-type additives in solar cells.[10] They found that despite the small size of the scaffold, DCFs were good electron acceptors, capable of undergoing two reversible one-electron reductions. We also recently described the serendipitous formation of a stable push−pull DCF possessing a strong, remarkably bathochromically shifted charge-transfer band (λ_{max} = 782 nm, ε = 27 500 M^{-1} cm^{-1}) and amphoteric redox behavior.[11,12] These findings compelled us to explore the preparation of new DCFs and their reactivity toward the CA−RE reaction.

Here, we report the preparation of tetra-alkynylated DCFs and compare their optoelectronic properties to those of the previously reported tetraphenylated derivative.[10a] We describe an unusual divergence in the regioselectivity of the CA−RE reaction between differently substituted DCFs, which is explained in a combined experimental and computational study, involving electron paramagnetic resonance (EPR) spectroscopy of their corresponding radical anions.

RESULTS AND DISCUSSION

Preparation of Tetraalkynylated DCFs. We first considered elongating the conjugated π-chromophore of the DCF scaffold through substitution with alkynes, as they are highly efficient at extending effective conjugation length.[13] In the work by Andrew et al., the most electronically interesting DCFs were accessed from a stable starting cyclopentadienone, which was condensed with malononitrile in a Lewis acid-promoted Knoevenagel reaction.[10a] We adopted this approach to the preparation of perethynylated DCFs (Scheme 1a), whose cyclopentadienone precursors are known to be stable and isolable.[14] From tetrakis[(triisopropylsilyl)ethynyl]cyclopenta-2,4-dienone **1a**, DCF **2a** was prepared in good yield as a stable, green solid. The structure was confirmed by single crystal X-ray analysis (Scheme 1b, see the Supporting Information (SI) for details). The bulky silyl groups on the acetylene appear to be important to stability. Starting from a tetraethynylated cyclopentadienone, in which the terminal triisopropylsilyl (TIPS) groups were replaced by smaller *tert*-butyl groups, condensation with malononitrile gave **2b** as a green solid in low yield, which decomposed to a brown solid in a couple of weeks. Our attempts to access terminally deprotected, tetraethynyl-DCF **2c** via removal of the TIPS groups of **2a** with n-Bu_4NF in THF unfortunately led to an unidentifiable and inseparable mixture, and no **2c** was found.

Optoelectronic Properties. With ethynylated DCF **2a** in hand, we then compared its electron-accepting ability to that of previously reported tetraphenyl-DCF **3** (Table 1).[10a] The electronic absorption spectrum of **2a** in CH_2Cl_2 features a weak absorption band at λ_{max} = 698 nm (ε = 480 M^{-1} cm^{-1}), which occurs at a much lower energy compared to **3** but with a similarly weak absorption strength (λ_{max} = 543 nm, ε = 400 M^{-1} cm^{-1}) (for the spectra, see the Supporting Information). DCF **2a** undergoes two reversible one-electron reductions in CH_2Cl_2 at −0.57 and −1.13 V (vs Fc/Fc^+); each occurs at more anodic potential than the corresponding reductions of **3**

Table 1. Optical and Electronic Properties of Compounds

compound	λ_{max}, nm[a] (ε, $M^{-1}cm^{-1}$)	E_{ox}, V[b]	E_{red}, V[b]
1a	559 (1890)	–	−0.90 −1.50
2a	698 (480)	–	−0.57 −1.13
2b	691 (670)	+1.19[c]	−0.71 −1.29
3[d]	543 (400)	–	−0.91 −1.50
4	721 (24 700)	+0.54	−0.78 −1.07
5	621 (23 900)	+0.73[c] +0.49	−1.04 −1.17
6	633 (23 600)	+0.60[c] +0.49[c]	−0.91 −1.08
7	453 (17 300)	+0.96 +0.70	−1.22 −1.38

[a]Measured in CH_2Cl_2 solution. [b]Values measured by CV in CH_2Cl_2 solution (+ 0.1 M NBu_4PF_6), v = 0.1 V s^{-1}. Values reported vs Fc/Fc^+. All values correspond to one-electron oxidation or reduction steps. [c]Irreversible peak potential. [d]Data from ref 10a.

Scheme 1. (a) Synthesis of 2a, 2b, and 3 and the Attempted Synthesis of 2c and (b) Crystal Structure of 2a at 100 K[a]

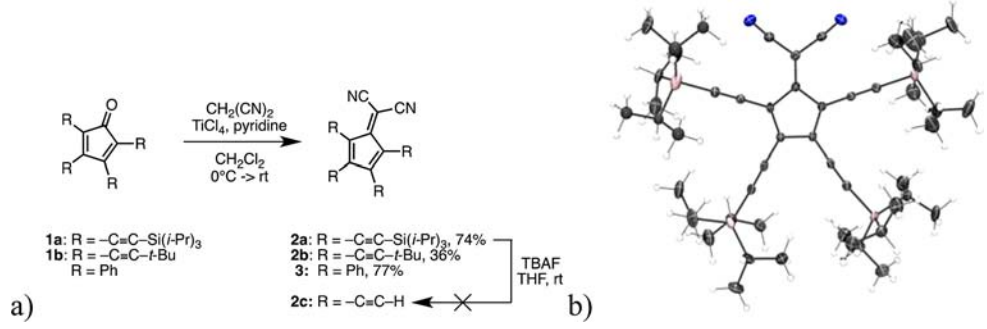

[a]Thermal ellipsoids shown at 50% probability.

(E_{red} = −0.91, −1.50 V vs Fc/Fc$^+$). *tert*-Butyl-substituted DCF **2b** also features two reversible one-electron reductions at slightly more cathodic potentials than **2a** (E_{red} = −0.71 V, −1.29 V vs Fc/Fc$^+$) and also displays irreversible oxidation at high potential (E_{ox} = +1.19 V vs Fc/Fc$^+$). We observe no oxidation waves in the cyclic voltammograms (CVs) of **2a** or **3**.

The electrochemistry of **1a** has not been previously reported, and its analysis reveals decisive insights to the electronic contribution of the alkyne substituents. The reduction pathways of many cyclopentadienones, such as tetraphenylcyclopentadienone, consist of a single two-electron reduction (E_{red} = −1.52 V vs Fc/Fc$^+$).[10a,15] By contrast, **1a** displays two reversible one-electron reductions. Clearly, ancillary substitution plays an important role in the electronics of these systems.

Figure 2 shows the calculated HOMO and LUMO energies (B3LYP/TZVP) for different fulvene derivatives. By far the lowest HOMO−LUMO gap is computed for tetraalkynylated **2a**. The effect of cyano substitution at C(6) is relatively simple to understand. Theory predicts that the LUMO should be stabilized by this substitution since the electron population is delocalized into the electron-withdrawing cyano groups.[7f,16] This is illustrated by the substantial decrease of the LUMO energy for 6,6-dicyanofulvene compared to fulvene (Figure 2). The effects of the tetraphenyl and tetrakis(TIPS-ethynyl) substitution are more complex, because there is a subtle interplay between the substituents on the cyclopentadiene ring and the cyano groups, particularly in the LUMO. Substitution on the cyclopentadiene ring also affects the HOMO strongly.

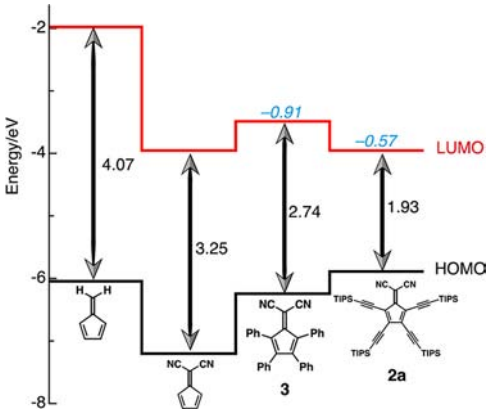

Figure 2. Calculated HOMO and LUMO energies (B3LYP/TZVP) of pentafulvene, DCF, **3**, and **2a**. The arrows and the corresponding numbers represent the HOMO−LUMO gap in eV. The blue numbers in italics are the experimentally determined (first) redox potentials (in V vs Fc/Fc$^+$).

EPR of Radical Anions. An experimental exploration of the LUMO structure of conjugated materials is best undertaken by EPR analysis of the one-electron reduced species.[17] The reversible first reductions detected at −0.57 and −0.91 V for **2a** and **3**, respectively, indicate that these derivatives should form rather persistent radical anions. Indeed, reduction (Na metal, THF) leads to intense EPR spectra.

Reduction of **2a** produces a well-resolved EPR spectrum (Figure 3) centered at the *g* factor of 2.0026. The main five-line signal pattern is produced by hyperfine coupling constants (hfcs) of the two equivalent ^{14}N nuclei (^{14}N hfc 0.13 mT, calcd 0.13 mT). The additional EPR lines of weaker intensity are produced by ^{29}Si satellite lines. Here, two ^{29}Si hyperfine

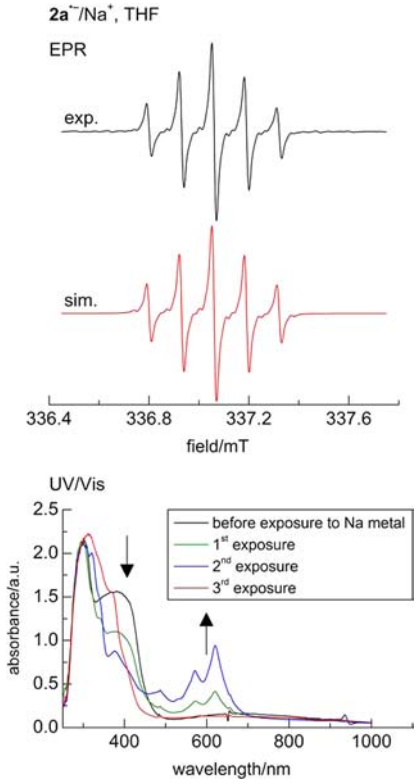

Figure 3. (top) EPR spectrum attributed to **2a**$^{\bullet-}$ (THF, 294 K) together with its simulation (taking into account ^{29}Si satellites) and (bottom) the corresponding UV−vis (MeTHF) spectra recorded during the reduction. Reductions are nonstoichiometric and imply fresh exposure to the Na mirror.

coupling constants of 0.11 and 0.06 mT (each for two ^{29}Si, calcd 0.12 and 0.08 mT, respectively) can be discerned. This shows that spin is also transferred onto the silyl substituents and explains their stabilizing effect in terms of lowering the reduction potential compared to **2b**. The reduction process of **2a** is accompanied with the occurrence of new absorptions in the visible region (green curve in Figure 3, new λ_{max} at 560 and 620 nm). Excessive reduction by multiple exposures to fresh Na mirror leads to the decay of these latter absorption bands and disappearance of the EPR signal. Freezing the sample to 77 K does not show any EPR spectrum, indicating that a triplet-state species is not likely formed.

The EPR signal attributed to **3**$^{\bullet-}$ is not resolved (Figure 4), but application of the ENDOR technique reveals three different isotropic ^{1}H hfcs of 0.05, 0.02, and 0.007 mT. According to DFT calculations, these hfcs can be assigned to the *ortho*- and *para*-protons (virtually equivalent hfcs (4 + 2) H) and the *meta*-protons (4 H) in the 3,4-phenyl groups and to the protons in the 2,5-phenyl substituents (10 H) of **3**$^{\bullet-}$. Together with a ^{14}N hfc of 0.13 mT (2 N) a simulation that matches the experimental spectrum can be obtained (Figure 4). The electron distribution represented by these hyperfine data is in good agreement with the calculated geometry, which has also been confirmed by X-ray structural analysis.[10a] The two phenyl substituents at C(2) and C(5) are oriented almost perpendicular toward the plane of the fulvene, while those at C(3) and C(4) are only tilted by ca. 50°. Accordingly, owing to the substantial orbital coefficients at C(3) and C(4) and the more coplanar arrangement of the phenyl groups, the charge and the spin are mainly delocalized into the two phenyl groups at C(3) and C(4).

dx.doi.org/10.1021/ja309141r | J. Am. Chem. Soc. 2012, 134, 18139−18146

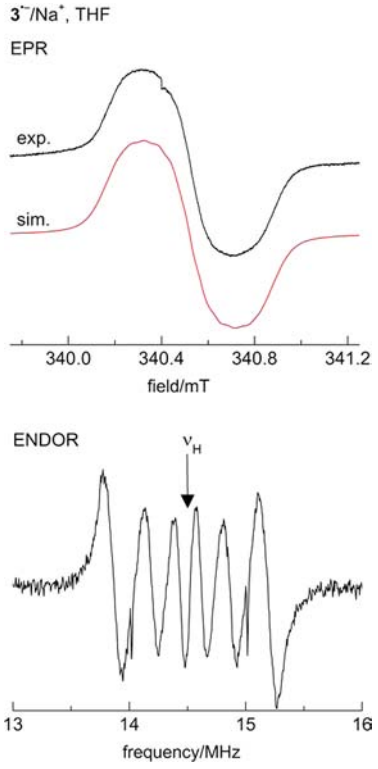

Figure 4. (top) EPR (experimental and simulated) spectra assigned to $3^{\bullet-}$ and (bottom) the corresponding ENDOR spectrum in THF.

In the context of the structure of the radical anions, it is noteworthy to compare the electron distribution and geometry in alkynylated **2a** and phenylated **3** and their one-electron reduced stages (B3LYP/TZVP) (Table 2SI). At the neutral stage, the bond lengths of the cyclopentadienyl ring in pentafulvene, DCF, and **2a** are typical for an alternating π-system [(C1)−C(2) and C(3)−C(4) 1.47−1.48 Å; C(2)−C(3) 1.35−1.38 Å]. In **3**, the calculated C(3)−C(4) distance reaches 1.51 Å with the adjacent bonds shortened, compared to **2a**, to 1.36 Å. Evidently, the two phenyl rings at C(3) and C(4) substantially contribute to electron delocalization in **3** (Figure 28SI). This effect is diminished in radical anion $3^{\bullet-}$. In addition, the phenyl-substituted derivative **3** displays a different charge distribution than alkynylated **2a**. In particular, this becomes apparent when comparing the partial atomic charges of **2a** and **3** (Figures 29SI and 30SI). At the parent neutral stage, C(1) is negatively polarized in **2a**, but it carries a slightly positive charge in **3**, pointing to the five-membered ring having a reduced cyclopentadienyl-anionic character. For the radical anion, the exocyclic C(6) in phenyl derivative $3^{\bullet-}$ carries a slightly negative charge, whereas in $\mathbf{2a}^{\bullet-}$ it is positively polarized (SI). This distinct charge separation helps to explain the reactivity profiles seen below for the CA−RE reactions.

CA−RE Reactivity with Electron-Rich Alkynes. When we heated DCF **2a** with 4-ethynyl-*N*,*N*-dimethylaniline to 80 °C in acetonitrile for 27 h, CA−RE adduct **4** was isolated as the exclusive product in 64% yield (Table 2a). Bis-anilino-substituted ethyne and buta-1,3-diyne react similarly to give adducts **5** (97%) and **6** (47%), respectively. In these cases, higher temperatures and microwave heating lead to faster product formation without decomposition.[18] Crystals of **5** suitable for X-ray analysis were grown, confirming the identity of the CA−RE product (Figure 5a).[19] In the case of **6**, only monoaddition was observed; the alkyne of **6** does not react with **2a** even at high temperatures.

Table 2a. Synthesis of Fulvenoid CA−RE Adducts from 2a

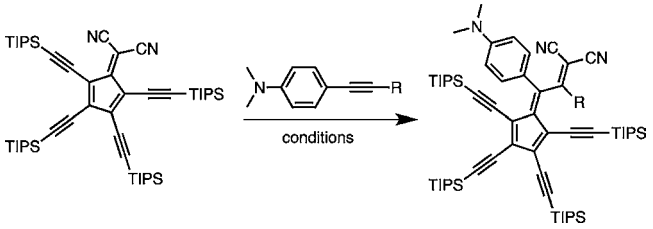

R	Solvent	Temp/°C	Time/h	Product	Yield/%
–H	MeCN	80	27	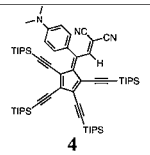 **4**	64
	MeCN/DCE (1:1)	160[a]	0.5	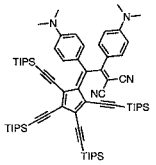 **5**	97
	MeCN/DCE (1:1)	160[a]	0.5	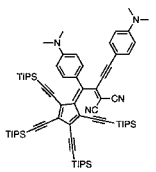 **6**	47

[a]Microwave heating.

dx.doi.org/10.1021/ja309141r | J. Am. Chem. Soc. 2012, 134, 18139−18146

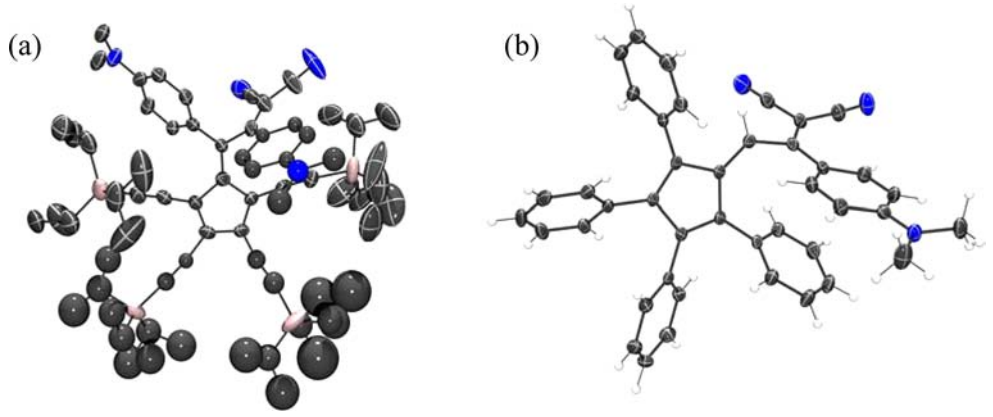

Figure 5. Crystal structures of (a) **5** (hydrogens omitted for clarity) and (b) **7** at 100 K. Thermal ellipsoids shown at 50% probability.

Table 2b. Synthesis of Fulvenoid CA−RE Adducts from 3

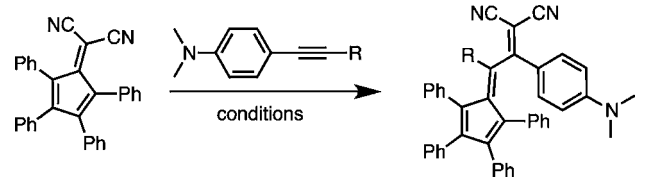

R	Solvent	Temp/°C	Time/h	Product	Yield/%
–H	MeCN	80	48	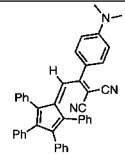 **7**	64
	MeCN/DCE (1:1)	80–200	1–24	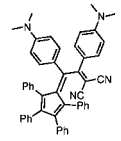	—[a]
	MeCN/DCE (1:1)	80–200	1–24	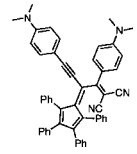	—[a]

[a]No reaction. Heating to 200 °C leads to decomposition of **3**.

Oddly, *t*-butylethynyl derivative **2b** decomposes upon reaction with electron-rich alkynes at room temperature to give unidentifiable mixtures. Push−pull chromophores **4**−**6** all feature strong, intramolecular charge-transfer (CT) bands that extend into the near-IR region, originating from the efficient conjugation from the anilino donor to the fulvene acceptor (Figure 11SI). The requirement of the aniline donor for intramolecular CT was demonstrated for push−pull chromophore **5** by treating a solution in CH_2Cl_2 with CF_3COOH, leading to attenuation of the CT band; the CT band reappeared when the acidified solution was treated with NEt_3 (Figure 13SI). Furthermore, **5** displays positive solvatochromism (Figure 14SI).

The regioselectivity of the CA−RE reaction to form **4**−**6** is identical to that previously observed in the transformations with TCNQ and *N*,*N*′-dicyanoquinone diimides (DCQNIs);[6d] that is, the anilino donor group is directly π-conjugated to the ring structure, enabling a proaromatic resonance structure in the acceptor ring.[20] The same proaromatic resonance is established in **4**−**6**, but this time with the five-membered cyclopentadiene ring.

We expected that tetraphenyl-DCF **3** would react with electron-rich alkynes similarly to **2a**. It does not. Heating **3** with 4-ethynyl-*N*,*N*-dimethylaniline in MeCN for 48 h at 80 °C leads exclusively to CA−RE adduct **7**, resulting from *opposite* regiochemistry in the CA−RE reaction (Table 2b). Bis-anilino-substituted alkynes do not react with **3**, even when heated to 200 °C in a sealed tube; decomposition of **3** is ultimately observed instead.

The UV−vis spectrum of **7** features a strong, hypsochromically shifted (compared to **3**) intramolecular CT band from the anilino donor to the dicyanovinyl acceptor (Figure 12SI, Supporting Information). The regiochemistry of **7** was confirmed by X-ray crystallographic analysis (Figure 5b). The anilino donor is now in direct linear π-conjugation with the adjacent dicyanovinyl group instead of the fulvene. The CV of **7** features two reversible one-electron reductions, which occur at more cathodic potentials compared to **3** as well as two one-electron oxidations at +0.70 and +0.96 V (vs Fc/Fc^+) (Table 1).

Mechanism of the CA−RE Reaction. While **7** is a rather unremarkable chromophore in and of itself, the *formation* of **7** was

dx.doi.org/10.1021/ja309141r | J. Am. Chem. Soc. 2012, 134, 18139−18146

Scheme 2. Reaction Pathways in the CA–RE Reaction with 6,6-Dicyanofulvenes

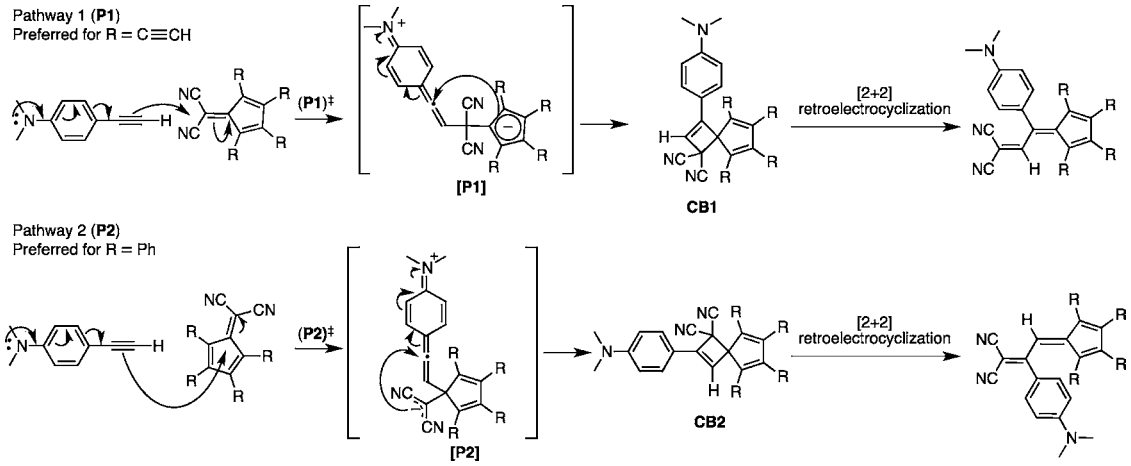

unexpected. This is the first time we have observed regioselectivity of this kind; when there is a choice between generation of a proaromatic structure and a structure with the donor in direct conjugation with a dicyanovinylidene unit, the proaromatic pathway has been preferred. More curious, still, is the fact that the substitution on the fulvene determines the regioselectivity of the CA–RE reaction. Previous work on the mechanism of the CA–RE reaction with dicyanovinyl acceptors[6b] led to the mechanisms proposed in Scheme 2.

The first step involves nucleophilic attack of the alkyne at the dicyanovinyl moiety to generate a zwitterionic intermediate. Because the site of initial nucleophilic attack is the arbiter of regioselectivity in this reaction, we focused our computational studies on the formation of the zwitterionic intermediate. Two potential reaction pathways are possible (Scheme 2). In Pathway 1 (**P1**), nucleophilic attack occurs at C(6) to generate the aromatic, zwitterionic intermediate. In Pathway 2 (**P2**), nucleophilic attack occurs at C(1) to generate an intermediate in which the negative charge is delocalized across the malononitrile moiety.

To gain insight into the observed regioselectivity, we turned to computational methods. Due to computational restrictions, calculations were performed with DCF **2c** instead of **2a**, at the wB97XD/6-31G(d)[21] level of theory, with polarizable continuum model (PCM) solvation in $CHCl_3$ (Gaussian 09, see SI for details). The calculated transition state (TS) and intermediate energies corroborate our empirical findings. For **2c**, pathway **P1** was lower in energy than **P2** for both TS ($\Delta\Delta G^{\ddagger}$ = 1.3 kcal mol^{-1}) and intermediate formation ($\Delta\Delta G$ = 3.4 kcal mol^{-1}) (Figure 31SI). In contrast, the computational results revealed that reaction of **3** preferred pathway **P2** over **P1** for both TS ($\Delta\Delta G^{\ddagger}$ = 4.0 kcal mol^{-1}) and intermediate formation ($\Delta\Delta G$ = 16.9 kcal mol^{-1}) (Figure 33SI).

The preference of tetraethynyl derivative **2c** for pathway **P1** seems to be the result of the additional efficient alkyne conjugation with the cyclopentadienyl ring. This extra conjugation, rather than aromaticity, appears to determine the regioselectivity of the reaction. The extra conjugation is supported by the EPR data of **2a**$^{\bullet-}$: strong hyperfine coupling to the terminal silicon atoms implies efficient communication across the alkynyl moieties. The site of attack on **2a** in pathway **P1** is at C(6), which carries a positive polarization in **2a**$^{\bullet-}$.

For **3**, computations and EPR data show that phenyl substitution, particularly at C(3) and C(4), reduces the anionic character on the cyclopentadienyl ring (see above). Atom C(1) in neutral **3** carries a distinctly positive charge, whereas the exocyclic C(6) in the radical anion carries a slightly negative charge. These data provide further support that attack at C(1), and thus pathway **P2**, is preferred.

■ CONCLUSION

We have synthesized a peralkynlated DCF **2a** and compared its electronic structure and properties to that of the previously investigated tetraphenylated DCF **3**. The enhanced susceptibility to one-electron reduction in **2a** is suggested by EPR analysis of the radical anions, showing that all ancillary silylalkynyl groups in **2a** participate in the stabilization of the radical anion, whereas in **3** the majority of the stabilization only results from the phenyl rings in the 3- and 4-position. Perethynylation completely changes the regioselectivity in the CA–RE reaction of 6,6-dicyanofulvenes with electron-rich alkynes, as compared to perphenylated analogues, thereby generating a new family of interesting push–pull chromophores. The electron transport properties are currently being studied, which should give insight into the utility of push–pull-substituted fulvenes in functional organic materials.

■ EXPERIMENTAL SECTION

General materials and physical characterization data can be found in the SI. Compounds **1a**,[14a] **1b**,[14a] **3**[10a] and 1,4-bis[(4′-*N*,*N*-dimethylamino)-phenyl]buta-1,3-diyne[22] were prepared according to literature procedures.

EPR Studies. *Chemical Reductions.* Reductions were performed in dry THF or MeTHF with the use of Na metal. THF was heated to reflux over Na/K alloy and stored over Na/K alloy under high vacuum. Benzophenone ketyl was used as an indicator for rigorously water-free conditions. Samples were prepared in a special three-compartment EPR sample tube connected to the vacuum line. Na metal mirror was sublimed to the wall of the tube, and about 0.4 mL of THF was freshly condensed to dissolve the investigated compound. The sample was successively degassed by three freeze–pump–thaw cycles and sealed under high vacuum. Reductions were performed by contact of the THF solution of the parent molecule with the Na metal mirror in the evacuated sample tube. The sample tubes were either stored at 190 K (isopropanol/dry ice bath) or immediately transferred into the microwave cavity of the EPR spectrometer. Each contact of the solution with the Na mirror leads to a stepwise reduction of the substrate by Na. Usually, after the initial short contact of the Na metal with the solution the EPR signal grows, and after additional contact, the signal decreases. This is due to the fact that primarily a basically quantitative one-electron reduction to the radical anion is achieved, then, gradually, the uptake of a second electron proceeds (such a behavior is illustrated in Figure 3).

EPR and ENDOR Measurements. EPR and ENDOR spectra were recorded using two ESP300 (Bruker, Germany) X-band spectrometers (one equipped with an ENDOR unit). Temperature control was achieved

dx.doi.org/10.1021/ja309141r | J. Am. Chem. Soc. 2012, 134, 18139–18146

using the EUROTHERM variable temperature units. Typical spectrometer settings for recording the solution EPR spectra were: microwave power = 0.2 mW, modulation amplitude = 0.015 mT, modulation frequency = 100 kHz, conversion time = 40.96 ms, time constant = 10.24 ms, and number of points = 2048. ENDOR spectra were recorded with microwave power = 10 mW, modulation amplitude = 0.1 mT, modulation frequency = 12.5 kHz, pump frequency = 10 MHz, modulation depth = 100 kHz and field locked at them maximum of the EPR line. Spectra were analyzed with WinEPR and SimFonia software provided by the spectrometers manufacturer as well as with WinSim,[23] a public domain program.

Synthesis of New Compounds. *2-{2,3,4,5-Tetrakis[(triisopropylsilyl)ethynyl]cyclopenta-2,4-dien-1-ylidene}malononitrile (**2a**).* A solution of **1a** (500 mg, 0.624 mmol) and malononitrile (82 mg, 1.24 mmol) in dry CH_2Cl_2 (10 mL) was cooled to 0 °C. $TiCl_4$ (0.35 mL, 3.11 mmol) was added dropwise, followed by dropwise addition of pyridine (1 mL). The solution was stirred at room temperature overnight. Water (20 mL) was added, the layers were separated, then the organic layer was washed with 10% aqueous HCl, dried over $MgSO_4$, and the solvent evaporated. Column chromatography (hexane/CH_2Cl_2 5:1) gave **2a** (0.392 g, 74%) as a green solid; mp 234 °C. ^{1}H NMR (400 MHz, $CDCl_3$) δ 1.14 (m, 84H, 4 Si($CHMe_2$)$_3$). ^{13}C NMR (101 MHz, $CDCl_3$) δ 159.04 (C), 138.64 (C), 120.42 (C), 115.49 (C), 111.36 (C), 110.62 (C), 100.14 (C), 96.86 (C), 86.02 (C), 18.87 (CH_3), 18.81 (CH_3), 11.68 (CH), 11.45 (CH). HR-MS (ESI+) $[M + H]^+$ calcd for $C_{52}H_{85}N_2Si_4$: 849.5784; found: 849.5766. IR (ATR) 2942 (m), 2890 (w), 2864 (m), 2187 (m), 2157 (w), 2104 (m), 1462 (m), 1427 (w), 1383 (m), 1354 (m), 1313 (w), 1231 (w), 1120 (w), 1074 (w), 1018 (m), 994 (m), 938 (m), 919 (w), 882 (s), 840 (m), 674 (s). UV–vis (CH_2Cl_2) λ_{max} (ε) 698 (480), 401 (16600). Anal. calcd for $C_{52}H_{84}N_2Si_4$: C, 73.51; H, 9.97; N, 3.30. Found: C, 73.22; H, 9.99; N, 3.39.

*2-[2,3,4,5-Tetrakis(3,3-dimethylbut-1-yn-1-yl)cyclopenta-2,4-dien-1-ylidene)malononitrile (**2b**).* A solution of **1b** (500 mg, 1.25 mmol) and malononitrile (165 mg, 2.50 mmol) in dry CH_2Cl_2 (20 mL) was cooled to 0 °C. $TiCl_4$ (0.69 mL, 6.25 mmol) was added dropwise, followed by dropwise addition of pyridine (2 mL). The solution was stirred at room temperature overnight. Water (20 mL) was added, the layers were separated, then the organic layer was washed with 10% aqueous HCl, dried over $MgSO_4$, and the solvent evaporated. Column chromatography (hexane/CH_2Cl_2 3:2) gave **2b** (0.200 g, 36%) as a green solid. Compound **2b** decomposed within a week in CH_2Cl_2 solution and over the course of several weeks as a solid. ^{1}H NMR (400 MHz, $CDCl_3$) δ 1.34 (s, 18H, 2 CMe_3), 1.32 (s, 18H, 2 CMe_3). ^{13}C NMR (101 MHz, $CDCl_3$) δ 160.72 (C), 138.87 (C), 119.44 (C), 118.39 (C), 112.89 (C), 111.67 (C), 83.99 (C), 75.00 (C), 71.64 (C), 30.79 (CH_3), 30.54 (CH_3), 29.29 (C), 29.07 (C). HR-MS (MALDI+) $[M]^+$ calcd for $C_{32}H_{36}N_2$: 448.2873; found: 448.2873. UV–vis (CH_2Cl_2) λ_{max} (ε) 691 (670).

*2-{2-[4-(Dimethylamino)phenyl]-2-[2,3,4,5-tetrakis((triisopropylsilyl)-ethynyl)cyclopenta-2,4-dien-1-ylidene]ethylidene}malononitrile (**4**).* Compound **2a** (85 mg, 0.1 mmol) and 4-ethynyl-*N*,*N*-dimethylaniline (14.5 mg, 0.1 mmol) were added to a 20 mL sealable vial with septum. The vessel was sealed, pumped, and purged with N_2 gas three times, and MeCN (1 mL) was added. The resulting suspension was stirred at 80 °C for 27 h. The solvent was removed by rotary evaporation. Column chromatography (hexane/CH_2Cl_2 3:2) gave **4** (64 mg, 64%) as a green solid; mp 220 °C (dec). ^{1}H NMR (400 MHz, $CDCl_3$) δ 8.71 (s, 1H), 7.15 (d, J = 8.9 Hz, 2H), 6.67 (d, J = 9.0 Hz, 2H), 3.10 (s, 6H), 1.21–1.09 (m, 64H), 0.94 (d, J = 7.2 Hz, 20H). ^{13}C NMR (101 MHz, $CDCl_3$) δ 161.60 (CH), 152.67 (C), 144.03 (C), 143.58 (C), 135.91 (CH), 135.00 (C), 134.47 (C), 125.51 (C), 122.01 (C), 119.98 (C), 113.92 (C), 111.94 (CH), 110.65 (C), 107.10 (C), 106.36 (C), 105.42 (C), 102.43 (C), 101.27 (C), 101.08 (C), 101.05 (C), 99.70 (C), 92.17 (C), 39.87 (CH_3), 18.83 (CH_3), 18.80 (CH_3), 11.77 (CH), 11.70 (CH). HR-MS (MALDI+) $[M]^+$ calcd for $C_{62}H_{95}N_3Si_4$: 993.6898; found: 993.6593. IR (ATR) 2942 (m), 2889 (m), 2863 (m), 2224 (w), 2120 (w), 1600 (s), 1540 (w), 1501 (s), 1460 (m), 1440 (m), 1370 (s), 1327 (m), 1232 (w), 1207 (w), 1186 (s), 1131 (w), 1097 (m), 1072 (w), 1017 (w), 995 (m), 983 (m), 945 (m), 920 (w), 882 (s), 837 (w), 816 (w). UV–vis (CH_2Cl_2) λ_{max} (ε) 721 (24700), 460 sh (14600), 381 (30800). Anal. calcd for $C_{62}H_{95}N_3Si_4$: C, 74.86; H, 9.63; N, 4.22. Found: C, 74.61; H, 9.45; N 4.25.

*2-{1,2-Bis[4-(dimethylamino)phenyl]-2-[2,3,4,5-tetrakis(triisopropylsilylethynyl)-cyclopenta-2,4-dien-1-ylidene]ethylidene}malononitrile (**5**).* A 2 mL microwave tube with septum cap was charged with **2a** (45 mg, 0.053 mmol) and 1,2-bis[(4′-*N*,*N*-dimethylamino)phenyl]ethyne (14 mg, 0.053 mmol). The tube was sealed, pumped, and purged with N_2 gas via a needle inserted through the septum, and MeCN (0.5 mL) and 1,2-dichloroethane (0.5 mL) were injected via syringe. The resulting suspension was heated to 160 °C for 30 min in the microwave. The solvent was evaporated, and purification by recycling preparatory GPC gave a metallic blue solid (57 mg, 97%); mp 266 °C (dec). ^{1}H NMR (600 MHz, $CDCl_3$) δ 7.64 (d, J = 9.1 Hz, 2H), 7.16 (br s, 2H), 6.53 – 6.44 (m, 4H), 2.99 (s, 6H), 2.97 (s, 6H), 1.04 (dd, J = 5.2, 2.3 Hz, 42H), 1.00 (d, J = 2.4 Hz, 12H), 0.92 (dd, J = 5.0, 2.2 Hz, 9H), 0.84 (t, J = 7.7 Hz, 18H), 0.74–0.64 (m, 3H). ^{13}C NMR (151 MHz, $CDCl_3$) δ 171.05 (C), 153.06 (C), 152.29 (C), 151.74 (C), 140.16 (C), 133.36 (CH), 133.29 (C), 133.16 (C), 126.95 (C), 123.05 (C), 121.79 (C), 120.72 (C), 116.00 (C), 114.11 (C), 111.49 (C), 111.26 (CH), 103.63 (C), 103.11 (C), 102.48 (C), 102.01 (C), 101.47 (C), 101.27 (C), 97.29 (C), 79.00 (C), 39.97 (CH_3), 39.83 (CH_3), 19.03 (CH_3), 18.88 (CH_3), 18.87 (CH_3), 18.82 (CH_3), 12.14 (CH), 11.93 (CH), 11.78 (CH), 11.60 (CH). Four signals, attributed to the aromatic carbons of the 4-(dimethylamino)phenyl ring attached to C(6) of the fulvene, are absent. This is likely due to rotation of the phenyl ring on the NMR time scale as evidenced in the ^{1}H NMR. HR-MS (MALDI) $[M + Na]^+$ calcd for $C_{70}H_{104}N_4NaSi_4$: 1135.7230; found: 1135.7227. IR (ATR) 2941 (m), 2863 (m), 2216 (w), 2122 (w), 1600 (s), 1493 (m), 1462 (m), 1437 (m), 1372 (s), 1330 (m), 1231 (w), 1206 (w), 1170 (s), 1088 (m), 1072 (m), 1017 (w), 984 (m), 944 (m), 881 (s), 816 (m), 783 (m), 766 (w), 753 (w), 719 (w), 673 (s). UV–vis (CH_2Cl_2) λ_{max} (ε) 621 (23900), 398 (30100). Anal. calcd for $C_{70}H_{104}N_4Si_4$: C, 75.48; H, 9.41; N, 5.03. Found: C, 75.20; H, 9.33; N 5.04.

*2-{1,4-Bis[4-(dimethylamino)phenyl]-1-[2,3,4,5-tetrakis(triisopropylsilylethynyl)-cyclopenta-2,4-dien-1-ylidene]but-3-yn-2-ylidene}-malononitrile (**6**).* A 2 mL microwave tube with septum cap was charged with **2a** (170 mg, 0.2 mmol) and 1,4-bis[(4′-*N*,*N*-dimethylamino)-phenyl]buta-1,3-diyne (29 mg, 0.1 mmol). The tube was sealed, pumped, and purged with N_2 gas via a needle inserted through the septum, and MeCN (0.5 mL) and 1,2-dichloroethane (0.5 mL) were injected via syringe. The resulting suspension was heated to 160 °C for 30 min in the microwave. Full conversion of the diyne to **6** was observed. The mixture was then heated in the microwave to 180 °C for 30 min in an attempt to induce reaction of the other alkyne, but no further reaction was observed. The solvent was evaporated, and purification by preparatory GPC gave **6** as a metallic blue solid (52 mg, 47%); mp 216 °C (dec.) ^{1}H NMR (600 MHz, CD_2Cl_2) δ 7.33 (d, J = 9.1 Hz, 2H), 7.31 (d, J = 9.1 Hz, 2H), 6.66 (d, J = 9.1 Hz, 2H), 6.62 (d, J = 9.1 Hz, 2H), 3.09 (s, 6H), 3.04 (s, 6H), 1.13 (d, J = 3.1 Hz, 45H), 1.06 (dd, J = 12.7, 7.2 Hz, 18H), 0.92 (dd, J = 7.4, 2.3 Hz, 18H), 0.83–0.72 (m, 3H). ^{13}C NMR (151 MHz, CD_2Cl_2) δ 155.49 (C), 153.60 (C), 152.91 (C), 148.27 (C), 140.74 (C), 137.55 (CH), 135.69 (CH), 133.40 (C), 133.19 (C), 125.55 (C), 122.84 (C), 121.21 (C), 121.06 (C), 114.88 (C), 112.93 (C), 112.04 (CH), 111.94 (C), 107.07 (C), 104.72 (C), 104.13 (C), 102.86 (C), 102.60 (C), 101.92 (C), 101.87 (C), 101.78 (C), 98.51 (C), 92.90 (C), 90.69 (C), 40.39 (CH_3), 40.33 (CH_3), 19.37 (CH_3), 19.31 (CH_3), 19.25 (CH_3), 19.18 (CH_3), 12.56 (CH), 12.43 (CH), 12.34 (CH), 12.19 (CH). HR-MS (MALDI) $[M + Na]^+$ calcd for $C_{72}H_{104}N_4Si_4$: 1159.7230; found: 1159.7225. IR (ATR) 2941 (m), 2863 (m), 2223 (w), 2143 (m), 1599 (s), 1529 (m), 1462 (m), 1441 (m), 1371 (m), 1223 (w), 1167 (m), 1115 (m), 1072 (w), 1017 (w), 995 (w), 941 (w), 881 (m), 816 (w), 800 (w), 779 (w), 762 (w), 721 (w), 674 (s). UV–vis (CH_2Cl_2) λ_{max} (ε) 633 (23600), 411 (29000). Anal. calcd for $C_{72}H_{104}N_4Si_4$: C, 75.99; H, 9.21; N, 4.92. Found: C, 75.73; H, 9.12; N, 4.88.

*2-{1-[4-(Dimethylamino)phenyl]-2-[2,3,4,5-tetraphenylcyclopenta-2,4-dien-1-ylidene]ethylidene}malononitrile (**7**).* Compound **3** (43 mg, 0.1 mmol) and 4-ethynyl-*N*,*N*-dimethylaniline (14.5 mg, 0.1 mmol) were added to a 20 mL vial with septum cap. The tube was sealed, pumped, and purged with N_2 gas twice, and MeCN (1 mL) was added via syringe, and heated to 80 °C for 48 h. The solvent was evaporated. Column chromatography (CH_2Cl_2/hexane 4:1) gave a red solid (37 mg,

64%); mp 280 °C (dec). ^{1}H NMR (400 MHz, $CDCl_3$) δ 7.47 (d, J = 9.2 Hz, 2H), 7.38−7.29 (m, 5H), 7.19−6.93 (m, 11H), 6.91 (s, 1H), 6.90−6.78 (m, 2H), 6.56 (d, J = 9.2 Hz, 2H), 3.10 (s, 6H). ^{13}C NMR (101 MHz, $CDCl_3$) δ 166.99 (C), 153.34 (C), 152.95 (C), 148.34 (C), 144.41 (C), 135.53 (C), 134.51 (C), 134.39 (C), 134.25 (C), 132.61 (CH), 132.07 (CH), 131.54 (C), 131.41 (CH), 130.52 (CH), 130.28 (CH), 130.23 (CH), 128.33 (CH), 127.64 (CH), 127.54 (CH), 127.32 (CH), 127.27 (C), 127.09 (CH), 121.50, 111.18 (CH), 40.14 (CH_3). HR-MS (MALDI) $[M + H]^+$ calcd for $C_{42}H_{32}N_3$: 578.2591; found: 578.2593. IR (ATR) 2922 (w), 2207 (m), 1603 (s), 1538 (w), 1483 (s), 1435 (m), 1412 (w), 1383 (m), 1338 (m), 1294 (w), 1211 (m), 1170 (m), 1114 (w), 1073 (w), 1025 (w), 908 (w), 821 (m), 812 (m), 673 (s). UV−vis (CH_2Cl_2) λ_{max} (ε) 453 (17300), 355 (18000). Anal. calcd for $C_{42}H_{31}N_3$: C, 87.32; H, 5.41; N, 7.27. Found: C, 85.63; H, 5.54; N, 7.16. We were unable to obtain satisfactory elemental analysis for this compound, despite multiple attempts.

■ ASSOCIATED CONTENT

Supporting Information

Synthesis and full characterization of new compounds, X-ray crystallographic data, coordinates for computational data. This data is available free of charge via the Internet at http://pubs.acs.org.

■ AUTHOR INFORMATION

Corresponding Author

diederich@org.chem.ethz.ch

Notes

The authors declare no competing financial interest.

■ ACKNOWLEDGMENTS

This work was supported by the ERC Advanced grant no. 246637 ("OPTELOMAC"). A.D.F. acknowledges the NSF−IRFP (U.S.A.) for a postdoctoral fellowship. O.D. thanks the Fonds der Chemischen Industrie (Germany) for a Kekulé fellowship. We thank Mr. Eirik Lyngvi for helpful discussions regarding computations.

■ REFERENCES

(1) (a) *Organic Light−Emitting Devices: Synthesis, Properties and Applications*; Müllen, K., Scherf, U., Eds.; Wiley-VCH: Weinheim, 2006. (b) *Organic Photovoltaics*; Brabec, C., Dyakonov, V., Scherf, U., Eds.; Wiley-VCH Verlag GmbH & Co. KGaA: Weinheim, Germany, 2008.

(2) (a) Paci, I.; Johnson, J. C.; Chen, X.; Rana, G.; Popovic, D.; David, D. E.; Nozik, A. J.; Ratner, M. A.; Michl, J. *J. Am. Chem. Soc.* **2006**, *128*, 16546−16553. (b) Henson, Z. B.; Müllen, K.; Bazan, G. C. *Nature Chem.* **2012**, *4*, 699−704.

(3) (a) Kivala, M.; Diederich, F. *Acc. Chem. Res.* **2009**, *42*, 235−248. (b) Kato, S.; Diederich, F. *Chem. Commun.* **2010**, *46*, 1994−2006.

(4) For examples of recent work by others, see: (a) Niu, S.; Ulrich, G.; Retailleau, P.; Ziessel, R. *Org. Lett.* **2011**, *13*, 4996−4999. (b) Shoji, T.; Ito, S.; Okujima, T.; Morita, N. *Eur. J. Org. Chem.* **2011**, 5134−5140. (c) Morimoto, M.; Murata, K.; Michinobu, T. *Chem. Commun.* **2011**, *47*, 9819−9821. (d) Leliège, A.; Blanchard, P.; Rousseau, T.; Roncali, J. *Org. Lett.* **2011**, *13*, 3098−3101. (e) Washino, Y.; Michinobu, T. *Macromol. Rapid Commun. Lett.* **2011**, *32*, 644−648.

(5) The group of Bruce has pioneered the chemistry of TCNE with alkyne−transition metal complexes. For a recent review, see: Bruce, M. I. *Aust. J. Chem.* **2011**, *64*, 77−103.

(6) (a) Jarowski, P. D.; Wu, Y.−L.; Boudon, C.; Gisselbrecht, J.−P.; Gross, M.; Schweizer, W. B.; Diederich, F. *Org. Biomol. Chem.* **2009**, *7*, 1312−1322. (b) Wu, Y.−L.; Jarowski, P. D.; Schweizer, W. B.; Diederich, F. *Chem.—Eur. J.* **2010**, *16*, 202−211. (c) Silvestri, F.; Jordan, M.; Howes, K.; Kivala, M.; Rivera−Fuentes, P.; Boudon, C.; Gisselbrecht, J.−P.; Schweizer, W. B.; Seiler, P.; Chiu, M.; Diederich, F. *Chem.—Eur. J.* **2011**, *17*, 6088−6097. (d) Chiu, M.; Jaun, B.; Beels, M. T. R.; Biaggio, I.; Gisselbrecht, J.−P.; Boudon, C.; Schweizer, W. B.; Kivala, M.; Diederich, F. *Org. Lett.* **2011**, *14*, 54−57.

(7) (a) Coulson, C. A.; Craig, D. P.; Maccoll, A. *Proc. Phys. Soc.* **1948**, *61*, 22−25. (b) Fukui, K.; Imamura, A.; Yonezawa, T.; Nagata, C. *Bull. Chem. Soc. Jpn.* **1960**, *33*, 1591−1599. (c) Baird, N. C. *J. Am. Chem. Soc.* **1972**, *94*, 4941−4948. (d) Ottosson, H.; Kilsa, K.; Chajara, K.; Piqueras, M. C.; Crespo, R.; Kato, H.; Muthas, D. *Chem.—Eur. J.* **2007**, *13*, 6998−7005. (e) Mitchell, R. H.; Zhang, R.; Berg, D. J.; Twamley, B.; Williams, R. V. *J. Am. Chem. Soc.* **2009**, *131*, 189−199. (f) Dahlstrand, C.; Rosenberg, M.; Kilsa, K.; Ottosson, H. *J. Phys. Chem. A* **2012**, *116*, 5008−5017.

(8) Brown, R. D.; Burden, F. R.; Kent, J. E. *J. Chem. Phys.* **1968**, *49*, 5542.

(9) (a) King, R. B.; Saran, M. S. *J. Chem. Soc., Chem. Commun.* **1974**, 851−852. (b) Junek, H.; Uray, G.; Zuschnig, G. *Liebigs Ann. Chem.* **1983**, 154−158. (c) Junek, H.; Uray, G.; Zuschnig, G. *Dyes Pigm.* **1988**, *9*, 137−152. (d) Katritzky, A. R.; Fan, W.−Q.; Liang, D.−S.; Li, Q.−L. *J. Heterocycl. Chem.* **1989**, *26*, 1541−1545.

(10) (a) Andrew, T. L.; Cox, J. R.; Swager, T. M. *Org. Lett.* **2010**, *12*, 5302−5305. (b) Andrew, T. L.; Bulovic, V. *ACS Nano* **2012**, *6*, 4671−4677.

(11) Jayamurugan, G.; Gisselbrecht, J.−P.; Boudon, C.; Schoenebeck, F.; Schweizer, W. B.; Bernet, B.; Diederich, F. *Chem. Commun.* **2011**, *47*, 4520−4522. The reactivity of this DCF derivative with electron-rich alkynes is complex and will be discussed elsewhere.

(12) A similar DCF was recently prepared as a byproduct of a secondary CA−RE reaction of an azulene-containing push−pull alkyne with TCNE: Shoji, T.; Ito, S.; Okujima, T.; Morita, N. *Org. Biomol. Chem.* **2012**, *10*, 8308−8313.

(13) Diederich, F. *Chem. Commun.* **2001**, 219−227.

(14) (a) Jux, N.; Holczer, K.; Rubin, Y. *Angew. Chem., Int. Ed. Engl.* **1996**, *35*, 1986−1990. (b) Tobe, Y.; Kubota, K.; Naemura, K. *J. Org. Chem.* **1997**, *62*, 3430−3431.

(15) Fox, M. A.; Campbell, K.; Maier, G.; Franz, L. H. *J. Org. Chem.* **1983**, *48*, 1762−1765.

(16) (a) Dahlstrand, C.; Yamazaki, K.; Kilsa, K.; Ottosson, H. *J. Org. Chem.* **2010**, *75*, 8060.

(17) (a) Kivala, M.; Stanoeva, T.; Michinobu, T.; Frank, B.; Gescheidt, G.; Diederich, F. *Chem.—Eur. J.* **2008**, *14*, 7638−7647. (b) Breiten, B. Jordan, M. Taura, D. Zalibera, M. Greisser, M.; Confortin, D.; Boudon, C.; Gisselbrecht, J.−P.; Schweizer, W. B.; Gescheidt, G.; Diederich, F. *J. Org. Chem.* **2012**, Article ASAP. DOI: 10.1021/jo301194y

(18) We do not ascribe any sort of special chemical reactivity to microwave irradiation; we merely find it to be a fast and safe method of heating, especially for heating solvents beyond their boiling point. Conventional heating gives similar results.

(19) It was not possible to grow X-ray quality crystals of **4** and **6**. This seems to be due in part to the highly disordered TIPS groups, which can be seen particularly in the crystal structure of **5**.

(20) Wu, Y.-L.; Bureš, F.; Jarowski, P. D.; Schweizer, W. B.; Boudon, C.; Gisselbrecht, J.-P.; Diederich, F. *Chem.—Eur. J.* **2010**, *16*, 9592−9605.

(21) This method accounts for favorable aromatic dispersion interactions. See: (a) Grimme, S. J. *J. Comput. Chem.* **2004**, *25*, 1463−1473. (b) Chai, J.−D.; Head−Gordon, M. *Phys. Chem. Chem. Phys.* **2008**, *10*, 6615−6620.

(22) Rodríguez, J. G.; Lafuente, A.; Martín-Villamil, R.; Martínez-Alcazar, M. P. *J. Phys. Org. Chem.* **2001**, *14*, 859−868.

(23) Duling, D. R. *J. Magn. Reson., B* **1994**, *104*, 105−110.